A letter to reply the comments

Title: Aqueous OH-initiated photooxidation of smoke extracts from maize straw and coal combustion: optical character and molecular composition

Dear editor

We thank very much for the valuable comments and suggestions from the reviewer, which is of great help to improve the quality of the manuscript. The comments were carefully considered and revisions have been made in response to suggestions. Following is our point-by-point responses to the comments and corresponding revisions.

Reviewer #1

1. Line 251-259, for the reported inorganic ion and transition metal measurements, it would be helpful to specify detection limits.

Response: Thanks for your helpful suggestion. We agree that providing the detection limits for inorganic ions and transition metals can improve analytical reliability of the measurements. In the revised manuscript, we have added the method detection limits for all reported inorganic ions and transition metals **in Section 2.3 (lines 152-154).** These detection limits were determined based on three times the standard deviation of blanks.

2. In Section 3.1, the manuscript reports changes in molecular weight and elemental composition during photooxidation, but it would be helpful to include a brief discussion on the possible mechanisms driving the different trends observed between coal and maize WSOM (e.g., why MW decreases in coal but remains stable in maize).

Response: Thanks for your valuable suggestions. We totally agree that the different trends in molecular weight (MW) evolution between coal- and maize-derived WSOM require clearer mechanistic interpretation. In revised manuscript **Line 440-456**, we added discussion such as: “At the molecular-class level, CHON compounds in maize smoke initially exhibit a relatively high average molecular weight (MW, 329.45 g/mol) and DBE (10.52). Upon photolysis, the average MW decreases to 301.07 g/mol (11 h) and 296.44 g/mol (23 h), while the DBE declines to 6.59 and 4.14, respectively. These changes reflect the progressive breakdown of conjugated structures and a corresponding reduction in aromaticity, consistent with the observed decrease in light absorbance (Fig.2 b). For coal smoke, a considerable fraction of CHONS species undergoes transformation into CHON compounds with lower aromaticity and DBE during photolysis. This conversion increases the relative abundance of CHON species while contributing to a decrease in overall molecular weight. In addition, the MW of CHO compounds in coal smoke decreases progressively with photolysis. In contrast, maize-smoke WSOM is dominated by CHO compounds, whose MW remains relatively unchanged during photolysis, resulting in only minor variation in the bulk molecular weight. This contrast primarily reflects differences in the initial WSOC compositions between coal and maize smoke. Overall, the marked decreases in AI and DBE for CHON compounds in both smokes indicate substantial loss of aromaticity, which in turn contributes to the reduction in light absorption."

3. In Section 3.3, the analysis of CHON compounds suggests different N-containing product formation between coal and maize WSOM. It would be useful to specify which types of N-containing compounds are likely responsible (e.g., nitroaromatic degradation products) and cite relevant literature to support this interpretation.

***Response*：** Thanks. We agree that the discussion of CHON compounds would benefit from a more specific identification of likely N-containing species and supporting literature. Previous study from Song et al. (2018) suggested that biomass burning smoke contain a high abundance of CHON species with oxidized nitrogen functional groups such as nitro compounds and/or organonitrates. In contrast, coal smoke enriched in aromatic organosulfates with high double bond equivalent (≥4). In the revised manuscript (**Section 3.3, lines 440-449**), we have expanded the discussion to specify the probable classes of N-containing compounds contributing to the observed CHON signals. **Such as:** At the molecular-class level, CHON compounds in maize smoke initially exhibit a relatively high average molecular weight (MW, 329.45 g/mol) and DBE (10.52). Upon photolysis, the average MW decreases to 301.07 g/mol (11 h) and 296.44 g/mol (23 h), while the DBE declines to 6.59 and 4.14, respectively. These changes reflect the progressive breakdown of conjugated structures and a corresponding reduction in aromaticity, consistent with the observed decrease in light absorbance (Fig.2 b). For coal smoke, a considerable fraction of CHONS species undergoes transformation into CHON compounds with lower aromaticity and DBE during photolysis. This conversion increases the relative abundance of CHON species while contributing to a decrease in overall molecular weight. **We have also incorporated relevant literature to support these assignments and pathways (Song et al., 2018).**

4. The manuscript reports changes in MW and elemental composition during photooxidation, but it would be helpful to include a brief discussion on the possible mechanisms driving the different trends observed between coal and maize WSOM (e.g., why MW decreases in coal but remains stable in maize).

Response： We totally agree with you. A clearer mechanistic explanation is needed to account for the different MW trends observed between coal- and maize-derived WSOM during photooxidation. These additions provide a more mechanistically grounded explanation for the observed differences and strengthen the interpretation of molecular evolution during aqueous-phase photooxidation. **In revised manuscript, we added more detailed explanation in many section,** including **Section 3.2, 3.6.2 and conclusion**.

5.The authors added 10 mM H_2O_2 to the reaction system, and therefore the conclusions mainly reflect the contribution of •OH radicals. It is suggested to discuss whether using a lower H_2O_2 concentration might lead to a greater contribution from singlet oxygen ($^1O_2$). The authors could consider including experiments with different H_2O_2 concentrations to examine the relative contributions of • OH, $^1O_2$, and $^3C^*$.

Response： We thank the reviewer for this insightful suggestion. We agree that the use of 10 mM H_2O_2 in our experiments favors the production of •OH and thus emphasizes •OH-driven oxidation pathways. In the revised manuscript, we have clarified that the selected H_2O_2 concentration was intended to ensure sufficient •OH generation within a practical experimental timescale and to enable systematic investigation of molecular transformation mechanisms. We have also expanded the discussionto address how different H_2O_2 concentration influence the relative importance of ROS. **The results are presented in Table S5**. **Added text descriptions were as follows** (**Section 3.6.1, lines 764–777**)**:** Surely, different H_2O_2 concentrations might influence the relative role of ROS. To assess this effect, we examined the ROS concentrations and their contributions under five different H_2O_2 levels (0.5, 1, 3, 5, and 10 mM). The results are presented in Table S5. As shown in Table S5, increasing the H_2O_2 dosage leads to higher •OH concentrations and relative contributions, accompanied by a corresponding decrease in the contribution of triplet excited states ($^3C^*$). The measured •OH concentrations generally fall within a relatively narrow range under five different H_2O_2 concentration, with average values of $(0.7-9.1)\times10^{-14}$ M and $(1.3-8.3)\times10^{-14}$ M, for coal and maize smoke WSOM, respectively. Specifically, we also noted that the $^1O_2$ contribution is only weakly affected by the H_2O_2 concentration. Given that this study mainly focuses on the role of •OH, all subsequent experiments were conducted at a relatively high H_2O_2 concentration. While additional experiments at varying H_2O_2 concentrations would provide valuable quantitative constraints on these processes, they are beyond the scope of the present study.

The following figure presents the detailed results of the supplementary experiment with 0.5 mM H_2O_2, which is used as a representative case to demonstrate the feasibility of conducting experiments with different H_2O_2 concentrations.

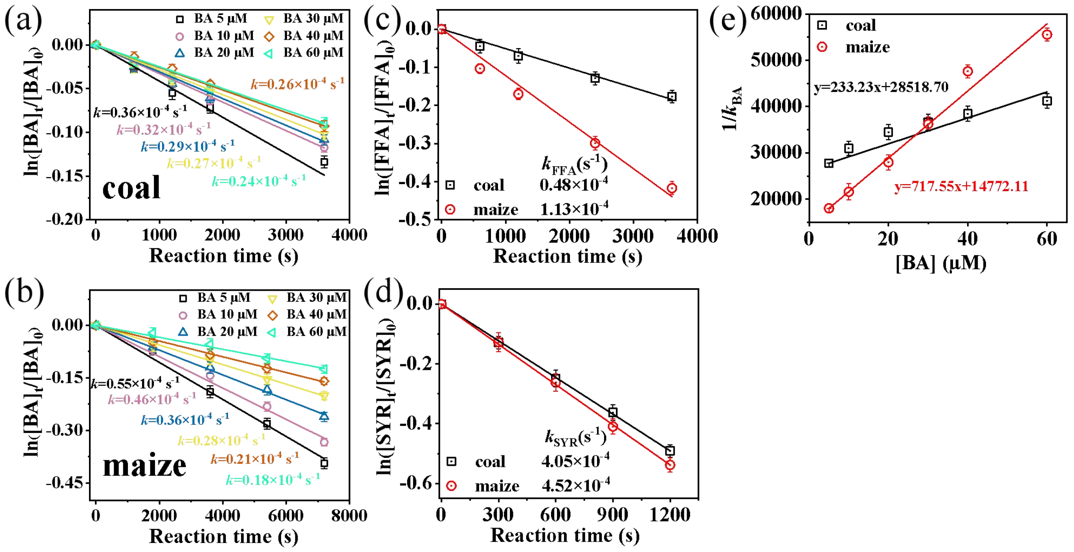

Figure Loss of (a, b) BA, (c) FFA, (d) SYR and (e)plot of $1/k_{BA}$ and BA concentration for two smoke WSOM under 0.5 mM H_2O_2 adding.

Table S5 Concentration and contribution to WSOM photodegradation of each ROS under different H_2O_2 concentration

Samples	$[H_2O_2]$ (mM)	[ROS] (M)			Contribution ratio (%)		
		$[\bullet OH]_{ss}$ ($\times 10^{-14}$)	$[^1O_2]_{ss}$ ($\times 10^{-13}$)	$[^3C^*]_{ss}$ ($\times 10^{-13}$)	•OH	$^1O_2$	$^3C^*$
coal	0.5	0.7	4.0	1.0	25.8	0.5	73.7
	1	1.6	3.4	1.0	46.6	0.3	53.1
	3	5.7	3.5	2.1	58.8	0.1	41.1
	5	8.7	4.1	2.6	63.5	0.1	36.4
	10	9.1	3.5	9.0	86.4	0.8	12.8
maize	0.5	1.3	9.4	1.2	37.2	0.8	62.0
	1	2.2	8.7	1.8	39.3	0.5	60.2
	3	3.8	2.5	1.3	60.9	0.1	39.0
	5	7.3	7.2	2.3	62.2	0.2	37.6
	10	8.6	0.2	7.1	80.9	3.1	16.0

6. Section 3.4: Lin 520-526, the authors employed HR–AMS to compare the temporal evolution of aqSOA produced from WSOM of two types of fuel combustion during aqueous-phase photochemical aging. They observed that the aqSOA yield from biomass was significantly lower than that from coal. It is recommended to relate these findings to the FT-ICR-MS results, rather than merely stating that the coal sample is more efficient at generating low-volatility species compared to maize."

Response: Thanks. We agree that the discussion of aqSOA formation would benefit from a more explicit linkage to the molecular-level information obtained from FT-ICR MS. In the revised manuscript**,** we have strengthened the discussion by connecting the higher aqSOA yield from coal-derived WSOM to its initial molecular composition **(Section 3.4, lines 555–564)**: The possible reasons why coal-derived aqSOA is higher than that from maize are as follows. First, the fresh coal-derived CHOS compounds are dominated by species such as $C_{17}H_{28}O_3S$ and $C_{18}H_{30}O_3S$, which are mainly organosulfates. These compounds have relatively high saturation and stability, and undergo little change upon photolysis, resulting in a high SOA mass yield measured by HR-AMS. In contrast, maize-derived WSOM is primarily composed of lignin-like substances with high DBE values, which are more susceptible to OH functionalization, forming saturated fatty acids or polyhydroxy acids (e.g., $C_9H_{18}O_6$ and $C_9H_{10}O_7$). These products can further undergo fragmentation into smaller, more volatile products (e.g., low-molecular-weight acids), leading to a lower aqSOA mass yield.

7.While the manuscript cites a substantial number of references, some interesting explorations conducted by researchers may be valuable for reference. However, these are all neglected by the authors, for example, Atmos. Chem. Phys., 20, 2513–2532, 2020; Environ. Sci. Technol. 2016, 50, 11815−11824

Response **:** Thanks for your suggestion. We appreciate the suggestion and have carefully reviewed the studies (Atmos. Chem. Phys., 20, 2513–2532, 2020; Environ. Sci. Technol., 2016, 50, 11815–11824), which provide important insights into aqueous-phase oxidation processes and the formation and evolution of organic aerosols. In the revised manuscript, we have incorporated these references into the Introduction and Discussion sections (**Section 3.2.2: lines 346; Section 3.3: line 423-424, 1014 and 1048**) to better contextualize our findings.

Specific Comments:

1.For the pie charts in Fig. 8, it is recommended to standardize the values and retain one decimal place throughout.

Response: Done.

2.The font size in the attached figures needs to be standardized, and there are some minor errors. For example, in the title of Table S4, 'Chemical properties and SOA mass yield of both coal-/maize-aqSOA,' there is a missing space between the words yield and of.

Response: Done.

3.Given that the properties of WSOM in both fuels can vary by region, it is recommended to specify their origin used in this study.

Response： Thanks. In the revised manuscript, we have provided the sources of both coal- and maize-derived samples in Section 2.2 "**Sample collection and experiment preparation", including that** "Coal and maize straw were collected from Lingwu (Ningxia) and Shangqiu (Henan Province), respectively, and combusted in a self-built stove designed to simulate domestic fuel burning conditions. Smoke particle collection followed the procedures described in our previous study (Ye et al., 2025).".

Reviewer #2

1.While the study presents a thorough analysis using advanced techniques, the mechanistic pathways for molecular transformations, especially the detailed role and interplay of ROS during photooxidation, require better elucidation. The manuscript should provide a more comprehensive discussion of likely chemical pathways and reactions influenced by ROS.

Response： We thank the reviewer for this important comment. We agree that the mechanistic pathways underlying molecular transformations, particularly the roles and interplay of different ROS, require a more comprehensive discussion.

In the revised manuscript, we **added Table S5 and S6 to present the top 10 most abundant compounds identified by FT-ICR MS** before photolysis and after 11 h and 23 h photodegradation, together with their DBE values, molecular formulas, inferred functional groups, and FT-ICR MS classifications. Then, a conceptual mechanism summarizing ROS-driven transformation pathways added in **Section 3.6.2.** Additionally, we have refined the conclusion section and supplemented it with a more detailed description of the ROS-driven reaction mechanisms **Line 868-876:** The contributions of ROS to photodegradation followed the order •OH > $^3C^*$ > $^1O_2$, highlighting the dominant role of •OH in aqueous-phase processing. Despite these common trends, distinct photochemical pathways were observed. Maize-derived WSOM exhibited more rapid oxidation during the early stage, likely driven by OH-functionalization reactions, whereas coal-derived WSOM showed greater compositional stability. Mechanistically, ROS promoted the conversion of lignin-like aromatics into highly oxygenated products via hydroxylation and ring-opening, while lipid-like compounds undergo functionalization and fragmentation. Secondary reactions with sulfate lead to the formation of organosulfates.

2.The manuscript mentioned transformations in molecular composition (e.g., decrease in aromaticity, increase in aliphatic components) without sufficient mechanistic backing. If the authors can provide more robust connections between analytical observations (e.g., FT-ICR MS results) and established chemical knowledge, it would improve the manuscript's depth.

***Response*：** Thanks for this valuable suggestion. We agree that the connections between the observed molecular transformations (e.g., decreases in aromaticity and increases in aliphatic components) and the underlying chemical mechanisms were not sufficiently developed in the original manuscript. In the revised version, we have strengthened the discussion by explicitly linking FT-ICR MS observations (e.g., changes in DBE, AI, MW) to established aqueous-phase oxidation mechanisms. We have strengthened the corresponding analyses in **Section 3.3** (Molecular composition of WSOM via FT-ICR MS), **Section 3.6.2**, **and the Conclusion,** thereby enhancing the overall depth of the manuscript. **Such as in conclusion Line 862-867:** Lignin-like compounds were progressively depleted, accompanied by an increase in lipid- and aliphatic-like species, suggesting the breakdown of conjugated structures and the formation of more saturated, oxygenated products. These transformations reduced chromophoric content through double-bond cleavage and aromatic ring opening, resulting in decreased light absorption and fluorescence.

3. More in-depth reasoning should be provided to explain the observed changes in optical properties (e.g., changes in MAE_{365}). Address potential uncertainties regarding how different molecular transformations (e.g., aromatic-to-aliphatic) contribute to these changes.

Response: We appreciate the reviewer's suggestion. In revised manuscript, we have strengthened the mechanistic interpretation linking molecular composition to optical properties **in Section 3.2.1 Line 329-336.** Specifically, our results indicate that lignin-like compounds, which are abundant in CHO and CHON classes in fresh maize smoke WSOM, are typically enriched in aromatic rings and π-conjugated structures that act as major chromophores responsible for near-UV light absorption. **Line 330-336:** The observed decrease in lignin-like fractions, together with reductions in DBE and AI values, suggests the breakdown of these conjugated systems during aqueous photooxidation, leading to a decline in MAE_{365}. Meanwhile, the formation of more saturated compounds (e.g., lipid- and aliphatic-like species) further contributes to the decrease in MAE_{365}. In addition, the formation of small oxygenated CHO species (e.g., carboxylic acids or CHO_2^+ fragments from HR-AMS) with negligible absorbance at 365 nm dilutes the overall light-absorbing capacity.

Overall, the observed changes in MAE_{365} likely reflect the combined effects of chromophore degradation, formation of weakly absorbing products, and potential generation of new light-absorbing species. The use of bulk parameters such as MAE_{365} inherently integrates contributions from complex mixtures, making it challenging to quantitatively apportion the contributions of individual molecular classes. For example, tot all CHO and CHON compounds contribute equally to light absorption, as chromophoric properties depend on factors such as conjugation length and functional group substitution.

4.The methods for quantifying ROS, such as •OH and $^1O_2$, using EPR warrant more detailed explanation. Specific conditions and potential limitations (e.g., resolution, calibration) should be elaborated.

Response : We thank the reviewer for this valuable comment. We agree that a more detailed description of the EPR-based quantification of ROS is necessary. In the revised manuscript, we have expanded the Methods section (**Section 2.7 ROS determination based on Electron paramagnetic resonance (EPR)**) to provide detailed information on the EPR measurements. Relevant details were presented in **Line 233-245**: Electron paramagnetic resonance (EPR) spectroscopy (Bruker EMXnano, Germany) was used to detect ROS. 5,5-Dimethyl-1-pyrroline N-oxide (DMPO) and 2,2,6,6-tetramethylpiperidine (TEMP) were used as spin-trapping agents for ꭃOH and $^1O_2$ to identify the DMPO-OH adducts (1:2:2:1) and the TEMPO adducts (1:1:1), respectively (Hu et al., 2025). The 10 mL of aqueous extracts were diluted into 100 mL using deionized water and pH was adjusted at 5.0 ± 0.1 with 0.1 M H_2SO_4 solutions. Then 100 mM of two spin-trapping agents were added into the 50 mL of acidified aerosol extract solutions. After photodegradation of WSOM extracts, 200 μL of solutions were transferred from the reaction solutions and immediately analyzed by EPR. The EPR parameters were set as following: modulation frequency of 100 kHz; center field of 3460 G, modulation amplitude of 1G, microwave power of 25 mW, sweep width of 200 G, sweep time of 150 s, number of scans of 20. **We also added references to support (Wang, J., Wang, S. Reactive species in advanced oxidation processes: Formation, identification and reaction mechanism, Chem. Eng. J., 401,126158, https://doi.org/10.1016/j.cej., 2020.1261582020).** Additionally, we also admitted the limitation of EPR for ROS quantification **in Line 656-661**: It should be noted that EPR-based spin-trapping methods have inherent limitations. For example, spectral overlap and background signals may affect the resolution and accuracy of peak assignment. Furthermore, certain short-lived or low-reactivity ROS may not be effectively captured by the selected spin traps. Therefore, the reported ROS contributions should be interpreted as semi-quantitative estimates rather than absolute concentrations.

5. Describe the assumptions and any limitations involved in employing chemical probes like benzoic acid and others for steady-state ROS concentrations. These details are crucial for assessing the robustness and reliability of the results.

Response: The second-order reaction rate constant between BA and ·OH is strongly dependent on pH value. **Line 671-682:** Under low pH conditions, benzoic acid predominantly exists in its molecular form (BA), whereas at high pH it is mainly present as the deprotonated species (benzoate, BA^{-}). These different forms exhibit distinct reactivity toward ·OH. According to the literature, when pH > 6, BA^{-} is the dominant species, with a rate constant $k_{BA-,OH} = 6.0 \times 10^{9}\ M^{-1}\ s^{-1}$; When pH < 4, the molecular form dominates, with $k_{BA,\ OH} = 1.8\times10^{9}\ M^{-1}\ s^{-1}$. For example, BA has a second-order rate constant with OH of $(5.9 \pm 0.5) \times 10^{9}\ M^{-1}\ s^{-1}$ at pH 7 **(Aqueous Phase Photo-oxidation of Brown Carbon Nitrophenols: Reaction Kinetics, Mechanism, and Evolution of Light Absorption, ACS Earth Space Chem. 2018, 2, 225−234).** In this study, the initial pH values of coal and maize samples were 6.79 and 5.83, respectively, which decreased to 5.77 and 5.08 after 23 h of irradiation. Overall, the pH of the solution was between 5–7 throughout the reaction. Therefore, we adopted the literature value $k_{BA,\ OH} = 5.1 \times 10^{9}\ M^{-1}\ s^{-1}$ (Lei et al., 2023) to calculate the steady-state concentration of BA. **The added contents were shown in Line 671-682** in revised manuscript.

6.Clarify whether the H_2O_2 concentrations used in the experiments reflect atmospheric conditions or are merely a lab convenience for ensuring sufficient OH radical presence. Discuss the implications of these concentrations on generalizing findings to real-world scenarios.

Response: We totally agree with you. In this study, H_2O_2 was primarily employed as a controlled precursor to generate sufficient •OH radicals within a reasonable experimental timescale, allowing us to systematically investigate the molecular transformation pathways and optical evolution of smoke-derived WSOM. Why we select 10 mM? Firstly, we added experimental results on how different H_2O_2 concentration influence the relative importance of ROS. To do this, we examined the ROS concentrations and their contributions under five different H_2O_2 levels (0.5, 1, 3, 5, and 10 mM). **The results are presented in Table S5** in revised manuscript. As shown, increasing the H_2O_2 dosage leads to higher •OH concentrations and its relative contributions. The measured •OH concentrations generally fall within a relatively narrow range under five different H_2O_2 concentration, with average values of (0.7

$-9.1)\times10^{-14}$ M and $(1.3-8.3)\times10^{-14}$ M, for coal and maize smoke WSOM, respectively. It is at the upper range of OH concentrations in cloud and fog water [1, 2]. We also provided references about H_2O_2 addition (1 mM, 3 mM and 10 mM) [1, 3].

[1]Rachel F. Hems and Jonathan P. D. Abbatt. Aqueous phase photo-oxidation of brown carbon nitrophenols: Reaction kinetics, mechanism, and evolution of light absorption, ACS Earth Space Chem., 2018, 2, 225-234.

[2]Arakaki T, Anastasio C, Kuroki Y, et al. A general scavenging rate constant for reaction of hydroxyl radical with organic carbon in atmospheric waters, Environ. Sci. Technol., 2013, 47 (15), 8196-8203.

[3]Zhao R, Lee A K Y, Huang L, et al. Photochemical processing of aqueous atmospheric brown carbon, Atmos. Chem. Phys., 2015, 15, 6087-6100.

Table S5 Concentration and contribution to WSOM photodegradation of each ROS under different H_2O_2 concentration

Sample	$[H_2O_2]$ (mM)	[ROS] (M)			Contribution ratio (%)		
		$[\bullet OH]_{ss}$ ($\times10^{-14}$)	$[^1O_2]_{ss}$ ($\times10^{-13}$)	$[^3C^*]_{ss}$ ($\times10^{-13}$)	•OH	$^1O_2$	$^3C^*$
coal	0.5	0.7	4.0	1.0	25.8	0.5	73.7
	1	1.6	3.4	1.0	46.6	0.3	53.1
	3	5.7	3.5	2.1	58.8	0.1	41.1
	5	8.7	4.1	2.6	63.5	0.1	36.4
	10	9.1	3.5	9.0	86.4	0.8	12.8
maize	0.5	1.3	9.4	1.2	37.2	0.8	62.0
	1	2.2	8.7	1.8	39.3	0.5	60.2
	3	3.8	2.5	1.3	60.9	0.1	39.0
	5	7.3	7.2	2.3	62.2	0.2	37.6
	10	8.6	0.2	7.1	80.9	3.1	16.0

7.Although distinct pathways and effects are noted, the comparative analysis between maize and coal smoke extracts needs strengthening. Discuss potential reasons for the observed differences in greater detail, grounded in the composition and typical environmental impacts of each smoke type.

Response: We thank the reviewer for this constructive suggestion. We agree that the comparative analysis between maize and coal smoke extracts can be further strengthened by providing a more detailed mechanistic interpretation based on their compositional differences and environmental relevance. At the end of **Section 3.6.2**, a discussion was added that integrates FT-ICR MS and ROS analyses to elucidate the transformation mechanisms of coal and maize. For example, **Line 812-825**: Next, by integrating FT-ICR MS and ROS analyses, we further compared the molecular transformation mechanisms of the two types of smoke. **Table S6 and S7 list the top 10 most abundant compounds identified by FT-ICR MS before photolysis and after 11 h and 23 h photooxidation**, together with their DBE values, molecular formulas, inferred functional groups, and FT-ICR MS classifications.

Table S6 The top 10 most abundant compounds identified in coal smoke WSOM by FT-ICR MS

Samples	DBE	Formula	Percentage (%)	Functional groups	FTIRC-MS category
coal 0 h	0.5	$C_{12}H_{26}O_4S$	3.44	organosulfate	lipid -like
	4.5	$C_{17}H_{28}O_3S$	2.97	organosulfate	lipid-like
	7.5	C12H12O5	1.94	aromatic compound	lignin-like
	4.5	$C_{18}H_{30}O_3S$	1.82	organosulfate	lipid -like
	4.5	$C_{16}H_{26}O_3S$	1.32	organosulfate	lipid -like
	1.5	$C_{16}H_{32}O_2$	1.20	fatty acid	lipid -like
	0.5	$C_{14}H_{30}O_5S$	1.03	hydroxy-organosulfate	lipid -like
	1.5	$C_{18}H_{36}O_3$	0.99	hydroxy fatty acid	lipid-like
	7.5	$C_{13}H_{14}O_5$	0.85	trimethoxybenzoic acid	lignin-like
	9.5	$C_{14}H_{12}O_6$	0.84	lignin-like dimer	lignin-like
coal 11 h	1.5	$C_{16}H_{32}O_2$	4.21	palmitic acid	lipid-like
	0.5	$C_{18}H_{39}NO_5$	2.09	hydroxy fatty acid amide	lipid-like
	1.5	$C_{18}H_{36}O_2$	1.91	octadecanoic acid	lipid-like
	4.5	$C_{18}H_{30}O_3S$	1.33	unsaturated organosulfate	lipid-like
	0.5	$C_{19}H_{40}O_6$	1.13	polyhydroxy nonadecane	lipid-like
	3.5	$C_{12}H_{20}O_3$	1.02	dodecadienoic acid	lipid-like
	4.5	$C_{17}H_{28}O_3S$	0.96	unsaturated organosulfate	lipid-like
	2.5	$C_{18}H_{34}O_3$	0.96	unsaturated fatty acid	lipid-like
	4.5	$C_{19}H_{32}O_3S$	0.85	unsaturated organosulfate	lipid-like
	1.5	$C_{18}H_{36}O_3$	0.81	hydroxyl octadecanoic acid	lipid-like
coal 23 h	0.5	$C_{16}H_{35}NO_2$	6.21	fatty amide	lipid-like
	4.5	$C_{14}H_{22}O$	5.80	alkyl acetophenone	lipid -like
	1.5	$C_{16}H_{32}O_2$	3.41	hexadecanoic acid	lipid -like
	0.5	$C_{18}H_{39}NO_3$	3.24	hydroxy fatty acid amide	lipid -like
	1.5	$C_{12}H_{24}O_2$	2.86	saturated fatty acid	lipid -like
	0.5	$C_{18}H_{39}NO_4$	2.73	organic nitrate	lipid -like
	0.5	$C_{12}H_{26}O_4S$	2.52	organosulfate	lipid -like
	0.5	$C_{20}H_{43}NO_5$	1.99	hydroxy organic nitrate	lipid-like
	5.5	$C_{17}H_{26}O_4$	1.91	dicarboxylic acids	lipid-like
	1.5	$C_{18}H_{36}O_2$	1.74	octadecanoic acid	lipid-like

Table S7 The top 10 most abundant compounds identified in maize smoke WSOM by FT-ICR MS

Samples	DBE	Formula	Percentage (%)	Functional groups	FTIRC-MS category
maize 0 h	5.5	$C_9H_{10}O_4$	9.56	vanillic acid	lignin-like
	6.5	$C_8H_6O_4$	4.63	Phthalic acid	lignin-like
	5.5	$C_{10}H_{12}O_4$	1.62	veratric acid	lignin-like
	5.5	$C_7H_7NO_4$	1.36	nitrobenzoic acid	lignin-like
	6.5	$C_9H_8O_3$	1.18	hydroxycinnamic acid	lignin-like
	5.5	$C_9H_{10}O_3$	1.16	vanillin	lignin-like
	10.5	$C_{18}H_{18}O_7$	0.81	guaiacyl dimer	lignin-like
	8.5	$C_{11}H_8O_3$	0.74	hydroxyanthraquinone	condensed aromatic
	6.5	$C_{10}H_{10}O_4$	0.71	ferulic acid	lignin-like
	6.5	$C_9H_8O_4$	0.66	polyphenols	lignin-like
maize 11 h	4.5	$C_{14}H_{22}O$	2.63	aromatic ketone	aromatic
	1.5	$C_{16}H_{32}O_2$	2.58	saturated fatty acids	lipid-like
	1.5	$C_{18}H_{36}O_2$	2.15	saturated fatty acids	lipid-like
	2.5	$C_{13}H_{25}NO_3$	2.04	n-hydroxytridecanamide	lipid-like
	0.5	$C_{12}H_{26}O_4S$	1.67	alkyl organosulfate	aliphatic
	1.5	$C_{12}H_{24}O_2$	1.50	lauric acid	aliphatic
	1.5	$C_9H_{18}O_6$	1.18	polyhydroxy nonanoic acid	carbohydrate
	5.5	$C_9H_{10}O_7$	0.96	hydroxyphthalic acid	tannin-like
	2.5	$C_{18}H_{34}O_3$	0.75	hydroxy unsaturated fatty acid	lipid-like
	3.5	$C_{17}H_{30}O_5$	0.74	polyhydroxy unsaturated fatty acids	lipid-like
maize 23 h	4.5	$C_{14}H_{22}O$	13.18	aromatic ketone	aromatic
	1.5	$C_{16}H_{32}O_2$	7.03	saturated fatty acids	lipid-like
	1.5	$C_{12}H_{24}O_2$	5.83	lauric acid	aliphatic
	1.5	$C_{18}H_{36}O_2$	5.26	saturated fatty acids	lipid-like
	0.5	$C_{12}H_{26}O_4S$	3.37	alkyl organosulfate	aliphatic
	2.5	$C_{18}H_{34}O_3$	2.99	unsaturated fatty acid	lipid-like
	0.5	$C_{16}H_{35}NO_2$	2.15	fatty acid amide	lipid-like
	7.5	$C_{28}H_{44}O_2$	1.81	ergosterol peroxide	lipid-like
	4.5	$C_{15}H_{24}O_3$	1.48	sesquiterpenic acid	lipid-like
	0.5	$C_{14}H_{30}O_5S$	1.32	hydroxyl organosulfate	lipid-like

In conclusion, we have thoroughly revised the manuscript. In particular, some figures have been improved for clarity and presentation, and the manuscript has been carefully edited to refine the language and correct grammatical issues. We sincerely appreciate your consideration of our revised submission.